# Probing predictions due to the nonlocal interface Hamiltonian: Monte Carlo simulations of interfacial fluctuations in Ising films

L. Pang,[1,*] D. P. Landau,[2,†] and K. Binder[3,‡]
[1]*Georgia Gwinnett College, Lawrenceville, Georgia 30043, USA*
[2]*Center for Simulational Physics, The University of Georgia, Athens, Georgia 30602, USA*
[3]*Institut für Physik, Johannes Gutenberg Universität Mainz, 55099 Mainz, Germany*

(Received 26 March 2019; published 8 August 2019)

Extensive Monte Carlo simulations have been performed on an Ising ferromagnet under conditions that would lead to complete wetting in a semi-infinite system. We studied an $L \times L \times D$ slab geometry with oppositely directed surface fields so that a single interface is formed and can undergo a localization-delocalization transition. Under the chosen conditions the interface position is, on average, in the middle of the slab, and its fluctuations allow a sensitive test of predictions that the effective interactions between the interface and the confining surfaces are nonlocal. The decay of distance dependent correlation functions are measured within the surface, in the middle of the slab, and between middle and the surface for slabs of varying thickness $D$. From Fourier transforms of these correlation functions a nonlinear correlation length is extracted, and its behavior is found to confirm theoretical predictions for $D > 6$ lattice spacings.

DOI: 10.1103/PhysRevE.100.023303

## I. INTRODUCTION

The theoretical understanding of interfaces between coexisting phases and their interaction with confining boundaries has been a long-standing challenge [1–8]. Thus, phenomena such as wetting and dewetting [3–8], droplet spreading at walls [3,4,8], capillary condensation in pores [1,2,7,9–14], and heterogenous nucleation [15–23] are still subjects of research. In spite of decades of research, many questions still are open.

A very popular concept treats the interface as an essentially infinitesimally thin dividing surface between the coexisting phases (Fig. 1) [1–8]. Here it is anticipated that by sufficient coarse-graining short-wavelength degrees of freedom are eliminated [24]. The configurations of the interface are described by a (smooth) single-valued function $z = \ell(x, y)$, describing its heights over some confining external (inert) wall in the $x$-$y$ plane. Thus, there are no overhangs of the interface, and all bulk fluctuations inside the bulk phases are completely eliminated. Thus, one describes the system (which now only exhibits long-wavelength interfacial fluctuations as its degrees of freedom) by the so-called "capillary wave" [25] Hamiltonian.

However, while the idea expressed in Fig. 1 is clearly very appealing, the extent to which this reduction of the problem is consistently feasible is still controversial (e.g., [26–28]). Even for a "free" interface (very far from any wall) it is clear that the description needs to be modified on short-length scales for which the bulk phases also exhibit nontrivial correlations (of the local density of the fluid, in the case of the vapor-liquid coexistence). As Höfling and Dietrich [26] put it, "the representation of a liquid-vapor interface by a two-dimensional manifold renders only an incomplete picture of this inherently three-dimensional object." This problem becomes even more severe when considering a second-order wetting transition, where a change of suitable parameters (e.g., temperature $T$, or strength of a local surface potential acting on fluid particles close to the wall, etc.) leads to a continuous unbinding of the interface from the wall [5–7]. Thus, the theory of critical wetting has been a subject of long-standing debate [26,29–42]. However, systems with short-range surface forces on the particles exhibiting a second-order transition are difficult to find experimentally [6], and much evidence on this problem stems only from Monte Carlo simulations of a nearest-neighbor lattice gas or Ising model with a local surface field $H_1$ [33,36,41–43]. But it is of great conceptional importance to understand what goes wrong when the standard capillary wave Hamiltonian, where the wall simply produces a local potential $V_{\rm wall}(\ell)$, is used.

A possible resolution of the problem was pointed out by Parry and co-workers [38–40,44,45] who suggested that the actual interaction between the interface [described by the variable $\{z = \ell(x, y)\}$] and the wall [described by the surface $z(x, y) = 0$] must be nonlocal. So the potential felt by the interface at the coordinates $x, y$ does not only depend on the height $z = \ell(x, y)$ at this point, but also the interfacial positions $\ell(x', y')$ at all the neighboring points in its environment. This nonlocality causes long-ranged interfacial interactions controlling the repulsion from the wall that are not modeled correctly when only the local wall potential is used.

However, discriminating between the concept of a local wall potential $V_{\rm wall}(\ell)$ acting on the interface in Fig. 1 and the concept of nonlocal interactions is a subtle matter, and this is the subject of the present paper. Monte Carlo simulations of interfacial fluctuations of thin Ising films with

*lpang@ggc.edu
†dlandau@hal.physast.uga.edu
‡kurt.binder@uni-mainz.de

 

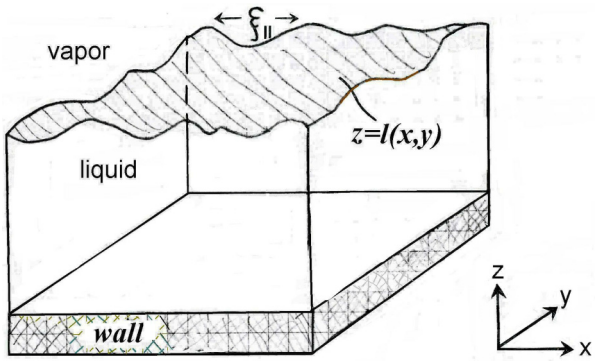


FIG. 1. Schematic illustration of the configuration of a coarse-grained interface (shaded) at local height $z = \ell(x, y)$ separating a liquid film at a wall from the vapor phase in thermal equilibrium at conditions where the phases can coexist in the bulk. The description in terms of the capillary wave Hamiltonian assumes that the only important degrees of freedom are smooth, long-wavelength undulations of the interface, with typical correlation length $\xi_{||}$, which is much larger than any molecular linear dimensions close to a second-order wetting transition.

competing walls permit the testing of specific consequences of the nonlocal theory. In the next section we shall sketch the theoretical background necessary to understand how this can be done. In Sec. III, we shall specify the simulation model and describe our results and their analysis. While preliminary results of this approach have been briefly described in a Ref. [46], this work suffered from an unfortunate choice of parameters, putting the system into the critical region of the second-order wetting transition (as a later study of critical wetting has revealed [42]) rather than in the region where complete wetting prevails. The present work uses conditions where this problem is avoided and also extends the study to significantly larger systems. Thus the finite-size effects, still quite visible in the preliminary work [46], now are essentially eliminated. Gratifyingly, the present work no longer suffers from some discrepancies between theoretical predictions and simulations, unlike [46]. Section IV then briefly summarizes our conclusions.

## II. THEORETICAL BACKGROUND

The capillary wave Hamiltonian that is normally used to describe the interfacial fluctuations of an interface interacting with a wall (Fig. 1) is

$$\mathcal{H}[\ell(x,y)] = \int dx \int dy \left[ \frac{\sum}{2} (\nabla \ell)^2 + V_{\rm wall}(\ell) \right], \qquad (1)$$

where $\sum$ is the interfacial stiffness, and $V_{\rm wall}$ describes the local wall potential which constrains the fluctuations of the local height $\ell(x, y)$ of the interface.

However, while a local potential is plausible for a point particle interacting with a wall, the interface is an extended object, and, as pointed out in the Introduction, a nonlocal interaction must be expected [38–40,44,47]. Parry *et al.* [44,45] constructed a systematic expansion for this nonlocal potential, and the leading-order diagrams of this diagrammatic expansion are depicted in Fig. 2. To be specific, the diagram

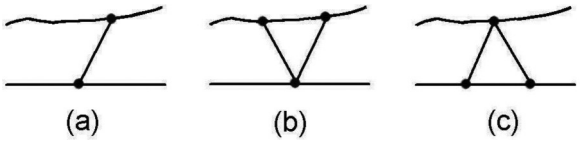


FIG. 2. Schematic illustration of the diagrams representing the leading-order contributions to the expansion of the nonlocal interaction between the wall (horizontal straight line) and the fluctuating interface (curved line).

of Fig. 2(a) represents a contribution

$$V_1 = \int dx \int dy \sqrt{1 + (\nabla \ell)^2}\, e^{-\kappa \ell(x,y)}, \qquad (2)$$

where $\kappa$ is of the order of the inverse correlation range in the bulk. The diagram of Fig. 2(b) corresponds to

$$V_2 = \int dx_1 \int dy_1 \int dx_2 \int dy_2\, U(x_{12}, \ell_{12}), \qquad (3)$$

where $x_{12}$ is the distance between the points $(x_1, y_1)$ and $(x_2, y_2)$ while $\ell_{12} = [\ell(x_1, y_1) + \ell(x_2, y_2)]/2$ and $U(x, \ell)$ is an isotropic two-body interfacial interaction.

For thick wetting films ($\kappa \ell_{12} \gg 1$) Eq. (3) can be rearranged as

$$V_2 \approx \int dx_1 \int dy_1 \int dx_2 \int dy_2\, e^{-\kappa \ell(x_1,y_1)} \times \frac{e^{-\kappa x_{12}^2/4\xi_{\rm NL}^2}}{4\pi \xi_{\rm NL}^2}\, e^{-\kappa \ell(x_2,y_2)}. \qquad (4)$$

Equation (4) involves the characteristic nonlocal correlation length of the Gaussian repulsion appearing in Eq. (4) as

$$\xi_{\rm NL} = \sqrt{\ell_{12}/\kappa}. \qquad (5)$$

This is a second parallel correlation length associated with interfacial fluctuations, in addition to the diverging length $\xi_{||}$ that is traditionally considered for critical wetting.

This description readily removes certain inconsistencies that appear when one works with only Eq. (1), such as violations of sum rules for correlation functions. The consequences of the nonlocal interface model are most easily explored for the case of "complete wetting," i.e., a system at temperatures where the fluid at liquid-vapor equilibrium would be above its wetting transition temperature, and slightly off bulk coexistence, so that the average distance $\bar{\ell}$ of the interface from the wall is much larger than all microscopic distances (which are of order $\kappa^{-1}$) but still finite. Nonlocality effects then show up in the site-site correlation $C(z_1, z_2, r)$ of the local order parameter at two sites at heights $z_1, z_2$ above the wall and separated by a radial distance $r$. For the liquid-vapor transition, the order parameter is the density difference between liquid and vapor. In the lattice-gas Ising model one simply studies the spin-spin correlations at the appropriate lattice sites. Specifically, we consider the Fourier transform [48]

$$G(z_1, z_2, \vec{q}) \approx \int dr_x \int dr_y\, \exp[i(q_x r_x + q_y r_y)] C(z_1, z_2, r), \qquad (6)$$

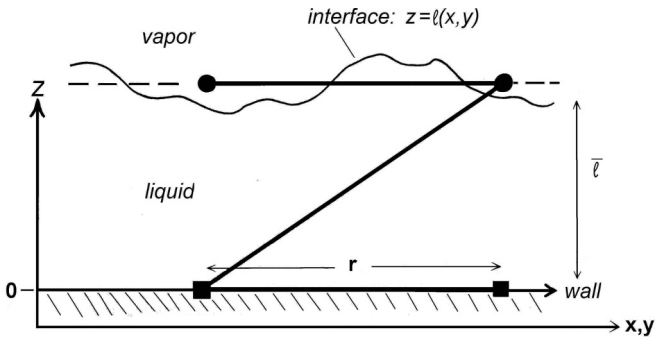


FIG. 3. (Schematic sketch of an interface at height $z = \ell(x, y)$ with average height $\bar{\ell}$ (broken horizontal straight line) above a wall at $z = 0$ (shaded). The thick straight line between points at the surface at distance $r$ indicated by squares indicates the correlation $C(0, 0, r)$, while the thick straight line between two points at distance $z = \bar{\ell}$ (circles) indicates the correlation $C(\bar{\ell}, \bar{\ell}, r)$. The third thick straight line connecting a point at the surface with a point at $z = \bar{\ell}$ represents the correlation $C(0, \bar{\ell}, r)$.

where $r_x, r_y$ are the $x, y$ coordinates of the distance vector $\vec{r}$, with $r^2 = r_x^2 + r_y^2$. Specifically, we consider three choices of $z_1, z_2$ (Fig. 3):

$$G(\bar{\ell}, \bar{\ell}, q) \propto (1 + q^2\xi_{||}^2)^{-1}, \tag{7}$$

$$G(0, \bar{\ell}, q) \propto \exp\big(-q^2\xi_{\rm NL}^2/2\big)/(1 + q^2\xi_{||}^2), \tag{8}$$

and

$$G(0, 0, q) \propto \exp\big(-q^2\xi_{\rm NL}^2\big)/(1 + q^2\xi_{||}^2). \tag{9}$$

Note that $G(z_1, z_2, q)$ in Eq. (6) always contains a regular background term and a term that becomes singular if $z_1$ and/or $z_2 = \bar{\ell}$ and $\bar{\ell}$ diverges [41]. Only the singular part is addressed in Eqs. (7)–(9). However, since $G(0, 0, 0)$ always stays finite, the singular part does not dominate $G(0, 0, q)$, and hence Eq. (9) is not useful for extracting the correlation lengths, hence $G(0, 0, q)$ will not be used further.

Equations (7)–(9) are supposed to hold in the regime of small wave numbers $q/\kappa \ll 1$, of course, and since [Eq. (5)] $\xi_{\rm NL}^2 = \bar{\ell}/\kappa$, the terms $q^2\xi_{\rm NL}^2 = q\bar{\ell}(q/\kappa)$ can be of order unity when $q\bar{\ell} \gg 1$. We recall that for complete wetting the dominating term of the wall potential $V_{\rm wall}(\ell)$ in the standard interface Hamiltonian is simply [cf. Eq. (2)] [5–7]

$$V_{\rm wall}(\ell) \propto \exp(-\kappa\ell), \tag{10}$$

so the effect of the nonlocal repulsion is felt under conditions where the effect of the local repulsion [Eqs. (2) and (10)] is rather weak.

Equations (1)–(10) all refer to a macroscopic system in a semi-infinite geometry ($z \geqslant 0$) whereas computer simulations, of course, can only be done for finite systems [49]. In $x$ and $y$ directions, use of a large parallel linear dimension $L \gg \xi_{||}$ and periodic boundary conditions makes the system quasi-infinite. However, the finiteness of the system in the $z$ direction, and the boundary condition for large $z$, is more subtle. In the framework of the Ising or lattice gas model, the wall at $z = 0$ in Figs. 1–3 is simply represented by a free boundary plane in which a surface field $H_1$ acts on the spins representing the occupancy of the lattice sites. Early

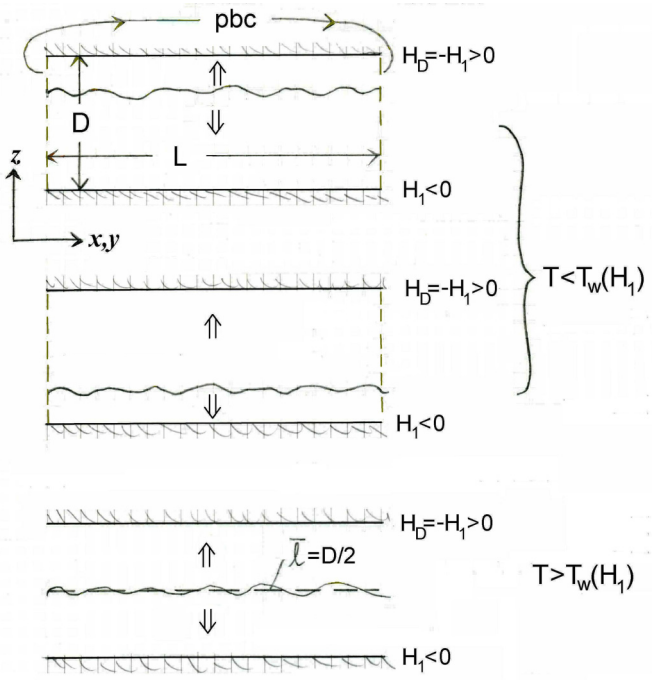


FIG. 4. Schematic view of an $L \times L \times D$ Ising system with antisymmetric surface fields $H_1 < 0$, $H_D = -H_1 > 0$, and periodic boundary conditions (pbc) in $x, y$ directions. The walls (free surfaces where surface fields act) at $z = 0, z = D$ are shaded. The signs of the magnetization in the domains separated by the interface (wavy line) are shown by thick arrows.

simulations of wetting transitions [33,36,43] then used a $L \times L \times D$ geometry with a second free boundary plane at $z = D$ and a surface field $H_D = H_1$. However, in the absence of a bulk field $H$ (with sign opposite to the sign of the surface fields) the state of the system with wetting layers on the walls (or precursors thereof) is only metastable, rather than truly thermodynamically stable. The proper stable situation of the system would be a state where the whole system is in the liquid phase (i.e., the "magnetization" of the spins in the bulk of the film has the same sign as the surface fields). Due to this problem, the estimation for the location of the wetting transition temperature $T_w(H_1)$ in this geometry (as done in [33,36,43]) is delicate. Recently [41,42] it was pointed out that choosing a strictly antisymmetric situation $H_1 = -H_D$ is more appropriate. Then, there is a single interface in the system, which in the regime of partial wetting [$T < T_w(H_1)$] is bound either to the wall at $z = 0$ or the wall at $z = D$, while in the wet region [$T > T_w(H_1)$] the interface fluctuates around the center of the film (Fig. 4), $\bar{\ell} = D/2$.

Strictly speaking, Fig. 4 applies only to the limiting case when both $D$ and $L$ are infinite, since otherwise the wetting transition is rounded by subtle finite-size effects [41,42]. If we choose $D$ finite and take only $L \to \infty$, we no longer have a wetting transition, but an interface localization or delocalization transition [47,50–53] occurs at $T_c(H_1, D)$, with $T_c(H_1, D \to \infty) \to T_w(H_1)$. Then the state for $T < T_c(H_1, D)$ is twofold degenerate, since the interface can be bound either to the wall at $z = 0$ or to the wall at $z = D$. For $T > T_c(H_1, D)$ the average interface position is at $\bar{\ell} = D/2$ (lower part of

Fig. 4). This is the analog of keeping the interface in the complete wetting regime at a distance $\bar{\ell} \propto \ln H$ by a bulk magnetic field. Since it was shown that $T_c(H_1, D)$ increases monotonically with increasing $D$ [52,53] hence $T_w(H_1)$ is approached from below as $D \to \infty$ choosing $T > T_w(H_1)$ is a sufficient condition for having $\bar{\ell} = D/2$. Thus, we can use Eqs. (7)–(9) when we study correlation functions indicated in Fig. 3 for the $L \times L \times D$ geometry with $\bar{\ell} = D/2$.

## III. SIMULATION RESULTS

Following Refs. [46,51–53] we study the nearest-neighbor Ising model in $L \times L \times D$ geometry (Fig. 4) on the simple cubic lattice, $J$ being the exchange constant,

$$\mathcal{H} = -J \sum_{\langle i,j \rangle} S_i S_j \quad - H_1 \sum_{i \in \text{layer } 1} S_i \quad - H_D \sum_{i \in \text{layer } D} S_i, \tag{11}$$

where $S_i = \pm 1$. We choose systems with $D = 6, 8, 10, 12, 14,$ and 16 layers, and the lateral linear dimension $L = 256$ and 512, with periodic boundary conditions throughout. Multiple runs are made with different starting configurations and different random number seeds to determine statistical errors and to detect any systematic errors. Typically, a total of around $10^8$ Monte Carlo steps per site were kept for computing averages of the correlation functions. We also keep the choice $|H_1|/J = 0.55$ consistent with previous work [46]. Note that it is important to choose the magnitude of the surface field such that the temperature $T$, which must be somewhat larger than $T_w(H_1)$, is neither close to the bulk critical temperature $T_{cb}$ [$J/k_B T_{cb} = 0.221\,654\,626(5)$ [54]] nor to the temperature of the interfacial roughening transition $T_R$ [$J/k_B T_R \approx 0.409(1)$ [55,56]]. In early work on wetting in the Ising model [36], it was concluded that for $J/k_B T = 0.25$, where the correlation length associated with bulk critical fluctuations is of the order of the lattice spacing and the lattice anisotropy of the interfacial tension is negligible [55–57], critical wetting occurs at $H_{1w}(T) \approx 0.55J$. Note that $H_{1w}(T)/J$ simply is the inverse function of $k_B T_w(H_1)/J$. Thus in our preliminary work [46] the inverse temperature $J/k_B T = 0.244$ was chosen, assuming hence that the choice ($J/k_B T = 0.244$, $|H_1|/J = 0.55$) is a state point in the wet region of the wetting phase diagram. However, recent work [42] has revealed that the early estimate $H_{1w}/J \approx 0.55$ for $J/k_B T = 0.25$ is too inaccurate, and actually $H_{1w}/J \approx 0.616$.

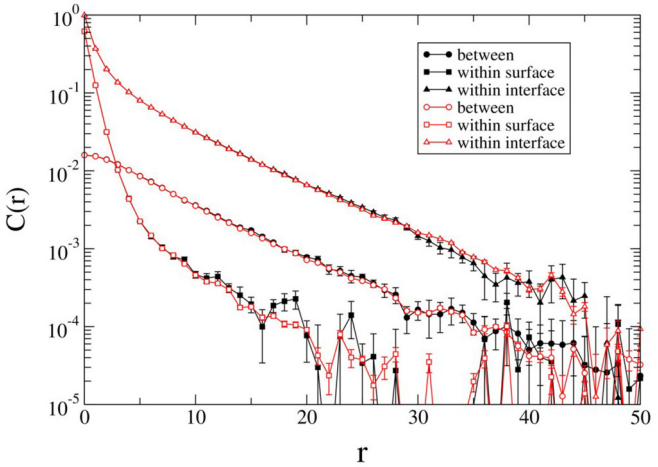


FIG. 5. Correlation functions $C(D/2, D/2, r)$ (top-most curves), $C(0, D/2, r)$ (curves in the middle), and $C(0, 0, r)$ (bottom curves) plotted vs $r$ for the case $D = 12$. Two data sets [for $L = 256$ (red open circles, squares, and triangles) and $L = 512$ (black closed circles, squares, and triangles)] are included in each case.

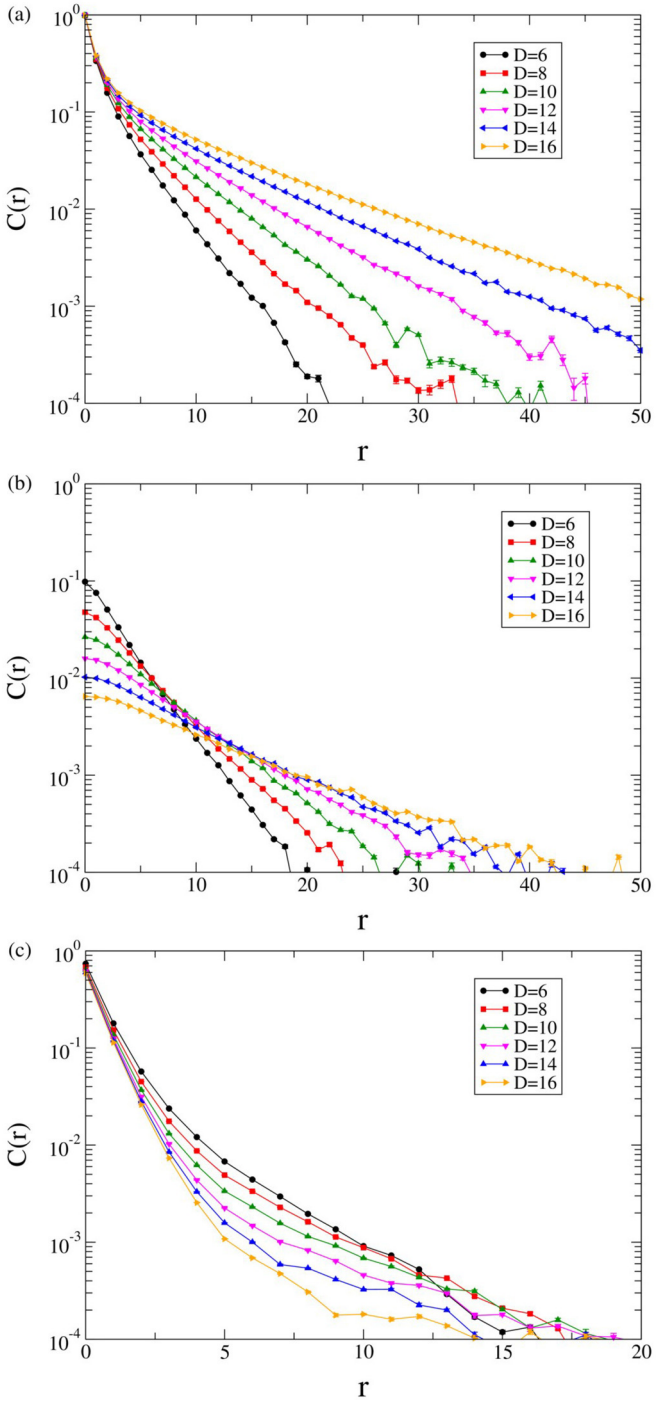


FIG. 6. Correlation functions (a) $C(\frac{D}{2}, \frac{D}{2}, r)$, (b) $C(0, \frac{D}{2}, r)$, and (c) $C(0, 0, r)$ plotted vs $r$ for the choice $L = 512$, $J/k_B T = 0.236$. Six choices of $D$ are included, as indicated.

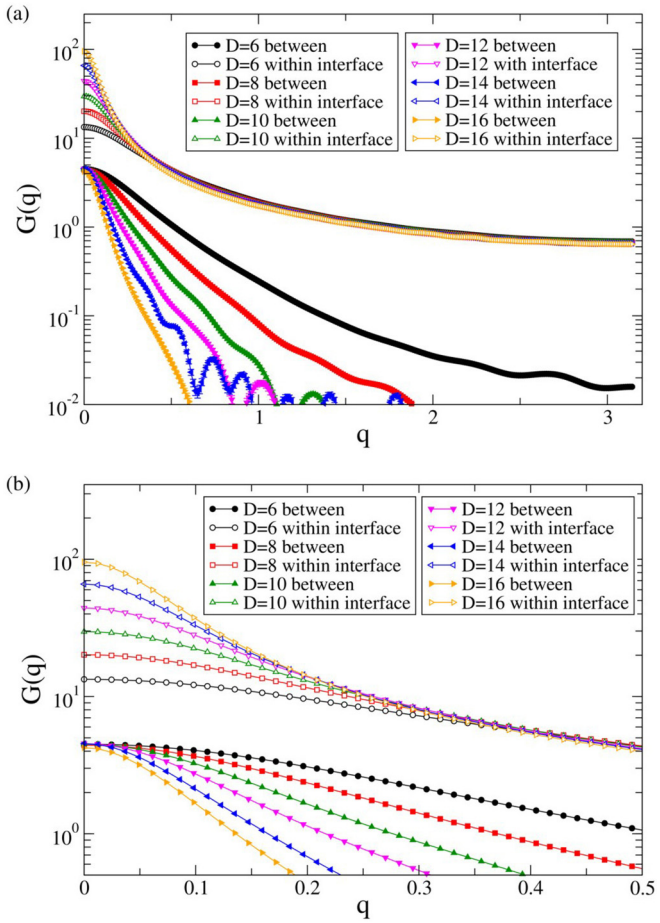


FIG. 7. Correlation functions $G(\frac{D}{2}, \frac{D}{2}, q)$ (upper set of curves) and $\mathbf{G}(0, \frac{D}{2}, q)$ plotted vs wave number $q$ for $L = 512$, $J/k_BT = 0.236$. Case (a) shows the full range $0 \leqslant q \leqslant \pi$ (note that our unit of length is the lattice spacing), case (b) shows the region of small $q$, to which the theoretical formulas [Eqs. (7) and (8)] should apply.

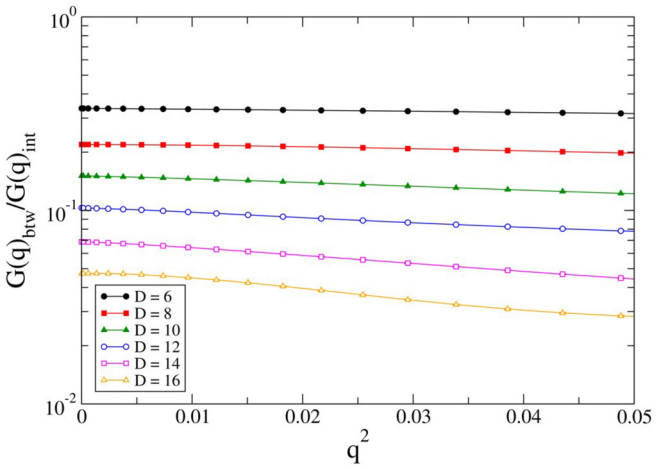


FIG. 8. Ratio of the correlation functions $G(0, D/2, q)/G(D/2, D/2, q)$ plotted vs $q^2$ for $L = 512$, $J/k_BT = 0.2360$, and several choices of $D$ as indicated. Note the logarithmic scale of the ordinate: straight lines indicate that the proposed variation proportional $\exp(-q^2\xi_{\rm NL}^2/2)$ holds.

The scaling relation [58] $H_{1w}/J = A(1 - T/T_{cb})^{\Delta_1}$ where the exponent $\Delta_1 \approx 0.48(3)$ [41,59] and the amplitude $A \approx 1.65$, leads to the conclusion that for $J/k_BT = 0.244$ the field $|H_1|/J = 0.55$ would coincide with $H_{1w}/J$ to within numerical error! This misjudgment of the location of the wetting transition explains why unusually large finite-size effects for $C(D/2, D/2, r)$ were detected in the preliminary work [46], thus making a meaningful estimation of $\xi_{||}$ impossible. Hence, in the present work we choose a temperature $J/k_BT = 0.236$ which is slightly closer to bulk criticality and for which $H_{1w}/J = 0.55$ is safely in the regime of complete wetting (irrespective of the remaining uncertainties in the exact location of the wetting transition phase boundary). A test for finite-size effects (Fig. 5) shows that the results are now indeed independent of $L$, to a very good accuracy. This figure is very different from its counterpart for $J/k_BT = 0.244$ (Fig. 2 in [46]) where strong size effects are apparent, rendering a meaningful estimation of $\xi_{||}$ impossible. Note that due to the discreteness of the lattice, distances $z$ are only possible at integer values $n = 1, 2, \ldots, D-1, D$. Here we measure all lengths in units of the lattice spacing.

Correlations for $z = 0$ actually refer to spins situated in the layer $n = 1$ above the lower wall. For an integer value of $D$, the actual midplane between the first ($n = 1$) and last ($n = D$) layer would actually fall in between the layers $n = D/2$ and $n = D/2 + 1$. So the correlation functions involving a point in the interface are always averages over points in both layers $\frac{D}{2}$ and $\frac{D}{2} + 1$,

$$C(z = D/2, z = D/2, r) \equiv \left[\tilde{C}\left(n = \frac{D}{2}, n = \frac{D}{2}, r\right) + \tilde{C}\left(n = \frac{D}{2} + 1, n = \frac{D}{2} + 1, r\right)\right]\Big/2, \tag{12}$$

$$C\left(z = 0, z = \frac{D}{2}, r\right) \equiv \left[\tilde{C}\left(n = 1, n = \frac{D}{2}, r\right) + \tilde{C}\left(n = 1, n = \frac{D}{2} + 1, r\right)\right]\Big/2. \tag{13}$$

where $\tilde{C}$ refers to the correlations between the discrete lattice points indicated within the parentheses. Since all correlations for small $r$ exhibit a nonexponential decay their analysis in real space would be difficult, although it is plausible that an exponential decay [proportional to $\exp(-r/\xi_{||})$] always takes over for large distances. This observation remains true for all choices of $D$ studied (Fig. 6).

Equations (7)–(9) suggest considering the Fourier transforms, and some such results are shown in Fig. 7. [Since $C(0, 0, r)$ only has good statistical accuracy for small $r$, where effects due to the length scale $\kappa^{-1}$ are still present, its Fourier transform is not considered here.]

Indeed the data for $G(\frac{D}{2}, \frac{D}{2}, q)$ have the shape expected for a simple Ornstein-Zernike type behavior that Eq. (7) suggests.

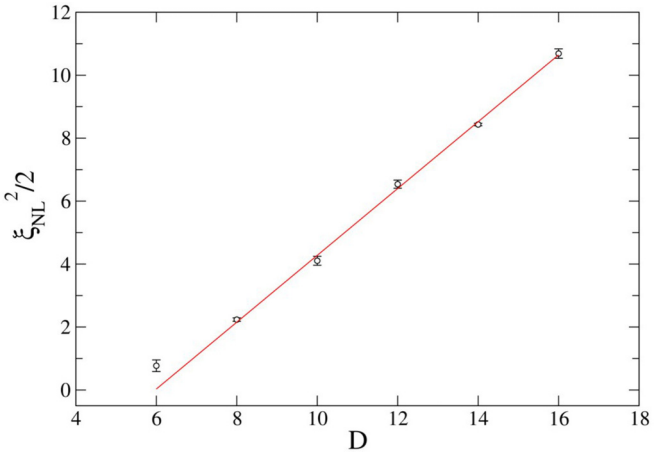


FIG. 9. Plot of nonlocal correlation length ($\xi_{NL}^2/2$) vs film thickness ($D$) for the choice $L = 512$, $J/k_BT = 0.236$.

In order to extract most conveniently the nonlocal correlation length $\xi_{NL}$, Eqs. (7) and (8) suggest analyzing the ratio $G(0, \frac{D}{2}, q)/G(\frac{D}{2}, \frac{D}{2}, q)$ since this should be proportional to a simple exponential decay $\exp(-q^2\xi_{NL}^2/2)$. Figure 8 provides evidence that this simple recipe actually works nicely for all $D > 6$ studied, and hence the decay constant $\xi_{NL}^2$ increases linearly with $D$. [Although the straight line does not intersect the origin for $D = 0$ but rather for $D = 6$. As should have been expected, the theory of Sec. II does not apply on length scales which are not much larger than $\kappa^{-1}$.]

The behavior of $\xi_{||}$ can be extracted from Eq. (7) and the prediction that $\xi_{||}(D) \propto \exp(\kappa D/4)$, and the data, shown in Fig. 10, verify this prediction. The rather modest values of $\xi_{||}$ indicate that, as anticipated, we were not too close to the critical wetting transition.

## IV. CONCLUSIONS

We have studied a long-standing, fundamental problem of statistical mechanics regarding the nature of a fluctuating interface interacting with a wall. Following decades of discussion about whether or not it could be viewed as a two-dimensional object subject to a potential due to the wall acting on this interface (see Fig. 1), Parry and co-workers [38–40,44,45] showed that such a description is possible provided the nonlocal character of the wall potential (see Fig. 2) is included. However, the direct consequences of this nonlocal interface are somewhat subtle and identifying them from quantities observable in experiments and simulations is challenging.

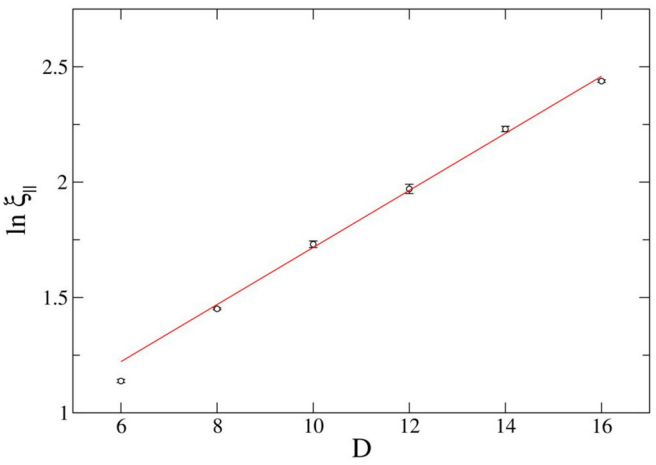


FIG. 10. Plot of parallel correlation length ($\ln\xi_{||}$) vs film thickness ($D$) for the choice $L = 512$, $J/k_BT = 0.236$.

In the present work, we have tested the prediction due to Parry *et al.* [41] that Fourier transforms of correlation functions probing fluctuations (Fig. 3) of an interface bound to the wall [Eqs. (6)–(8)] are described in terms of two mesoscopic lengths if the mean distance of the interface from the wall is much larger than molecular dimensions. For short-range forces, the larger of these lengths [which is already present for a strictly local interface potential $V(\ell)$] grows exponentially with this mean distance. The second length, due to the nonlocality of the potential, only grows with the square root of this distance.

In our preliminary Monte Carlo study of this problem [46] we exploited the idea that this behavior could be studied by choosing an Ising model with two competing planar surfaces a distance $D$ apart with antiparallel surface fields. The temperature was above the wetting transition temperature where the average interface distance from either wall is $D/2$ (Fig. 4). However, due to an unfavorable choice of temperature, the system was so close to the wetting transition that the results were hampered by strong finite-size effects associated with the parallel linear dimension $L$. Consequently, only qualitative evidence for the nonlocal theory was obtained.

The present work chose conditions that did not suffer from size effects so that the decay of the correlations could be determined accurately over three decades (Figs. 5 and 6). As a result, both correlation lengths could be extracted from the Fourier transforms, varying $D$ from 6 to 16 lattice spacings, for $L = 512$ (Figs. 7 and 8). Note that the slowness of long-wavelength interfacial fluctuations still precludes the choice of significantly larger values of $D$. Nevertheless, we are able to convincingly verify the theoretically expected variation of both correlation lengths with $D$ (Figs. 9 and 10). We thus feel that the present work presents comprehensive evidence for the nonlocal interface Hamiltonian theory.

## ACKNOWLEDGMENTS

L.P. thanks the Center for Simulational Physics at the University of Georgia for its hospitality. D.P.L. thanks the Alexander von Humboldt Foundation and the Graduiertenschule Materials Science in Mainz for support and the Institut für Physik at the Johannes Gutenberg Universität Mainz for its hospitality. This work was supported in part by resources from the Georgia Advanced Computing Resource Center, a partnership between the University of Georgia's Office of the Vice President for Research and Office of the Vice President for Information Technology.

[1] J. S. Rowlinson and B. Widom, *Molecular Theory of Capillarity* (Clarendon, Oxford, 1982).
[2] *Fluid Interfacial Phenomena*, edited by C. A. Croxton (Wiley, New York, 1986).
[3] P. G. de Gennes, F. Brochard, and D. Quéré, *Capillarity and Wetting Phenomena* (Springer, Berlin, 2004).
[4] P. G. de Gennes, Rev. Mod. Phys. **57**, 827 (1985).
[5] S. Dietrich, in *Phase Transitions and Critical Phenomena*, edited by C. Domb and J. L. Lebowitz (Academic, London, 1988), Vol. 12, p. 1.
[6] D. Bonn and D. Ross, Rep. Prog. Phys. **64**, 1085 (2001).
[7] K. Binder, D. P. Landau, and M. Müller, J. Stat. Phys. **110**, 1411 (2003).
[8] D. Bonn, J. Eggers, J. Indekeu, J. Meunier, and E. Rolley, Rev. Mod. Phys. **81**, 739 (2009)
[9] M. E. Fisher and H. Nakanishi, J. Chem. Phys. **75**, 5857 (1981).
[10] R. Evans, J. Phys.: Condens. Matter **2**, 8989 (1990).
[11] K. Binder and D. P. Landau, J. Chem. Phys. **96**, 1444 (1992).
[12] L. D. Gelb, K. E. Gubbins, R. Radhakrishnan, and M. Sliwinska-Barkoviak, Rep. Prog. Phys. **62**, 1573 (1999).
[13] M. Schoen and S. H. L. Klapp, Rev. Comput. Chem. **24**, 1 (2007).
[14] D. Wilms, A. Winkler, P. Virnau, and K. Binder, Phys. Rev. Lett. **105**, 045701 (2010).
[15] M. Volmer, *Kinetik der Phasenbildung* (Th. Steinhoff, Dresden, Leipzig, 1939).
[16] D. Turnbull, J. Appl. Phys. **21**, 1022 (1950).
[17] D. Turnbull, J. Chem. Phys. **18**, 198 (1950).
[18] G. Navascues and P. Tarazona, J. Chem. Phys. **75**, 2441 (1981).
[19] V. Talanquer and D. W. Oxtoby, J. Chem. Phys. **104**, 1483 (1996).
[20] T. V. Bykov and X. C. Zheng, J. Chem. Phys. **117**, 1851 (2002).
[21] A. Cacciuto and D. Frenkel, Phys. Rev. E **72**, 041604 (2005).
[22] D. Winter, P. Virnau, and K. Binder, Phys. Rev. Lett. **103**, 225703 (2009).
[23] M. L. Trobo, E. V. Albano, and K. Binder, J. Chem. Phys. **148**, 114701 (2018).
[24] J. D. Weeks, J. Chem. Phys. **67**, 3106 (1977).
[25] F. P. Buff, R. A. Lovett, and F. H. Stillinger, Phys. Rev. Lett. **15**, 621 (1965).
[26] F. Höfling and S. Dietrich, Europhys. Lett. **109**, 46002 (2015).
[27] E. Chacon and P. Tarazona, J. Phys.: Condens. Matter **28**, 244014 (2016).
[28] A. O. Parry, C. Rascon and R. Evans, J. Phys.: Condens. Matter **28**, 244013 (2016).
[29] E. Brézin, B. I. Halperin, and S. Leibler, Phys. Rev. Lett. **50**, 1387 (1983).
[30] R. Lipowsky, D. M. Kroll, and R. K. P. Zia, Phys. Rev. B **27**, 4499(R) (1983).
[31] D. S. Fisher and D. A. Huse, Phys. Rev. B **32**, 247 (1985).
[32] R. Lipowsky and M. E. Fisher, Phys. Rev. Lett. **57**, 2411 (1986).
[33] K. Binder, D. P. Landau, and D. M. Kroll, Phys. Rev. Lett. **56**, 2272 (1986).
[34] R. Lipowsky and M. E. Fisher, Phys. Rev. B **36**, 2126 (1987).
[35] T. Halpin-Healy and E. Brézin, Phys. Rev. Lett. **58**, 1220 (1987).
[36] K. Binder, D. P. Landau, and S. Wansleben, Phys. Rev. B **40**, 6971 (1989).
[37] A. O. Parry and C. J. Boulter, Phys. Rev. E **53**, 6577 (1996).
[38] A. O. Parry, J. M. Romero-Enrique, and A. Lazarides, Phys. Rev. Lett. **93**, 086104 (2004).
[39] A. O. Parry, C. Rascón, N. R. Bernardino, and J. M. Romero-Enrique, Phys. Rev. Lett. **100**, 136105 (2008).
[40] A. O. Parry, J. M. Romero-Enrique, N. R. Bernardino, and C. Rascón, J. Phys.: Condens, Matter **20**, 505102 (2008).
[41] E. V. Albano and K. Binder, Phys. Rev. Lett. **109**, 036101 (2012).
[42] P. Bryk and K. Binder, Phys. Rev. E **88**, 030401(R) (2013).
[43] K. Binder and D. P. Landau, Phys. Rev. B **37**, 1745 (1988).
[44] A. O. Parry, C. Rascón, N. R. Bernardino, and J. M. Romero-Enrique, J. Phys.: Condens. Matter **18**, 6433 (2006).
[45] A. O. Parry, C. Rascón, N. R. Bernardino, and J. M. Romero-Enrique, J. Phys.: Condens. Matter **19**, 416105 (2007).
[46] L. Pang, D. P. Landau, and K. Binder, Phys. Rev. Lett. **106**, 236102 (2011).
[47] A. O. Parry and R. Evans, Phys. Rev. Lett. **64**, 439 (1990).
[48] There is a misprint of the corresponding expression of [46] in the arguments of the exponential function.
[49] D. P. Landau and K. Binder, *A Guide to Monte Carlo Simulation in Statistical Physics*, 4th ed. (Cambridge University Press, Cambridge, UK, 2015).
[50] A. O. Parry and R. Evans, Phys. A (Amsterdam, Neth.) **181**, 250 (1992).
[51] K. Binder, D. P. Landau, and A. M. Ferrenberg, Phys. Rev. Lett. **74**, 298 (1995).
[52] K. Binder, D. P. Landau, and A. M. Ferrenberg, Phys. Rev. E **51**, 2823 (1995).
[53] K. Binder, R. Evans, D. P. Landau, and A. M. Ferrenberg, Phys. Rev. E **53**, 5023 (1996).
[54] A. M. Ferrenberg, J. Xu, and D. P. Landau, Phys. Rev. E **97**, 043301 (2018).
[55] K. K. Mon, S. Wansleben, D. P. Landau, and K. Binder, Phys. Rev. B **39**, 7089 (1989).
[56] M. Hasenbusch and K. Pinn, Phys. A (Amsterdam, Neth.) **192**, 342 (1993).
[57] B. J. Block, S. Kim, P. Virnau, and K. Binder, Phys. Rev. E **90**, 062106 (2014).
[58] H. Nakanishi and M. E. Fisher, Phys. Rev. Lett. **49**, 1565 (1982).
[59] H. W. Diehl, Int. J. Mod. Phys. B **11**, 3503 (1997).